ACS Sustainable Chemistry & Engineering

pubs.acs.org/journal/ascecg

Research Article

Production of Hexane-1,2,5,6-tetrol from Biorenewable Levoglucosanol over Pt-WO_x/TiO_2

Paolo Cuello-Penaloza, Siddarth H. Krishna, Mario De bruyn, Bert M. Weckhuysen, Edgard A. Lebrón-Rodríguez, Ive Hermans, James A. Dumesic, and George W. Huber*

Cite This: *ACS Sustainable Chem. Eng.* 2021, 9, 16123−16132

Read Online

ACCESS | Metrics & More | Article Recommendations | Supporting Information

ABSTRACT: We have investigated the synthesis of hexane-1,2,5,6-tetrol (hereafter "tetrol") from aqueous solutions of biomass-derived levoglucosanol (hereafter "Lgol") using a (10 wt %)Pt-(10 wt %)WO_x/TiO_2 catalyst in both batch and continuous flow reactors. The tetrol selectivity was over 90% with Lgol feed concentrations of 10−30 wt %. Most of the Lgol feed stereochemistry was preserved (notably 91%), with threo-Lgol (hereafter "t-Lgol") and erythro-Lgol (hereafter "e-Lgol") converting to (*S*,*S*)-tetrol and (*S*,*R*)-tetrol, respectively. The rate of Lgol conversion was found to be first-order in the Lgol concentration, suggesting that the catalyst surface is not saturated with Lgol. The measured reaction order for H_2 was zero, which is consistent with either a mechanism involving acid-catalyzed irreversible C−O bond cleavage of Lgol followed by metal-catalyzed hydrogenation of reactive intermediates or one where all of the metal sites are saturated with H_2. When the reaction was run in a continuous flow reactor, the catalyst exhibited deactivation with increasing time-on-stream but was found partially regenerable with a consecutive calcination and reduction treatment. Deactivation was concluded to be caused mainly by carbon deposition, with some W-leaching from the catalyst in the initial stages of reaction. The here demonstrated understanding of reaction kinetics and catalyst stability could facilitate the development of improved processes to produce hexane-1,2,5,6-tetrol from biomass.

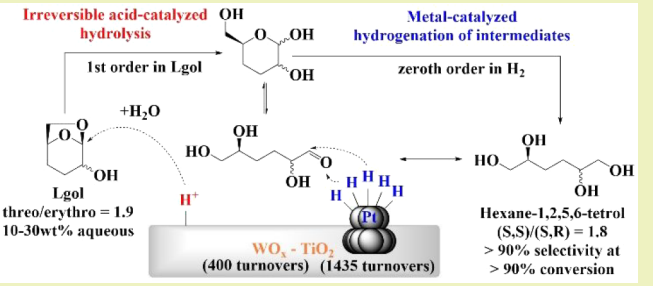

KEYWORDS: *biomass conversion, bifunctional acid-metal solid catalysts, levoglucosenone and derivates, polymer precursors, scalable processes, stereochemistry preservation, reaction orders, catalyst stability, activation energy*

INTRODUCTION

Channeling the production of commodity chemicals from petroleum-derived resources to renewable lignocellulosic feedstocks is a great route to the effective transitioning of the chemical industry toward materials and products with a lower CO_2 footprint. Biomass-derived monomers can be used as important platform molecules for the synthesis of polymers, resins, solvents, surfactants, among others.[1−9] Sugar derivatives have been shown to offer many opportunities to obtain such platform molecules.[10,11] Levoglucosenone (LGO) is a biobased sugar-like compound, which can be produced from cellulose by mild pyrolysis.[12−14] Notably, based on the pyrolytic method developed by the Circa Group, an actual 1000 ton LGO/year plant is currently being developed in France.[15] LGO can also be produced at yields up to 51% using polar aprotic solvents and sulfuric acid at 170−230 °C.[16] LGO is a highly functionalized molecule that can be used in asymmetric synthesis,[2,3] to create chiral pure pharmaceutical intermediates,[4,5] and for the synthesis of chemicals useful to the creation of polymers, such as hydroxymethylfurfural[1,6] (HMF). It has equally been established that dihydrolevoglucosenone (Cyrene) obtained from LGO hydrogenation[17] is a benign low-toxicity polar aprotic solvent with similar properties as dimethylformamide (DMF) or *N*-methylpyrrolidone (NMP).[7,9,18,19] Also, when adding Cyrene to water, a powerful hydrotrope is created, the central aspect to this phenomenon being Cyrene's geminal diol.[20] Other potentially useful LGO-derived molecules are Lgol,[17,21,22] tetrahydrofuran-dimethanol[22,23] (THFDM), hexane-1,2,6-triol (HTri),[24,25] hexane-1,6-diol[22,25−29] (1,6-HD), and tetrol.[28,30] The main reactants and products of interest for this work are shown in Figure 1.

Our group has recently demonstrated how Lgol can be selectively converted into tetrol.[30] Tetrol is a polyol of industrial interest,[29,31,32] which could be potentially useful to the synthesis of a range of polymers.[8,31] Also, since the molecule displays two chiral centers, it can have potential uses as a chiral synthon.[29] Tetrol is obtained by the selective C−O

Received: July 14, 2021
Revised: November 9, 2021
Published: November 19, 2021

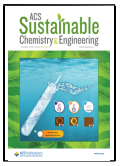

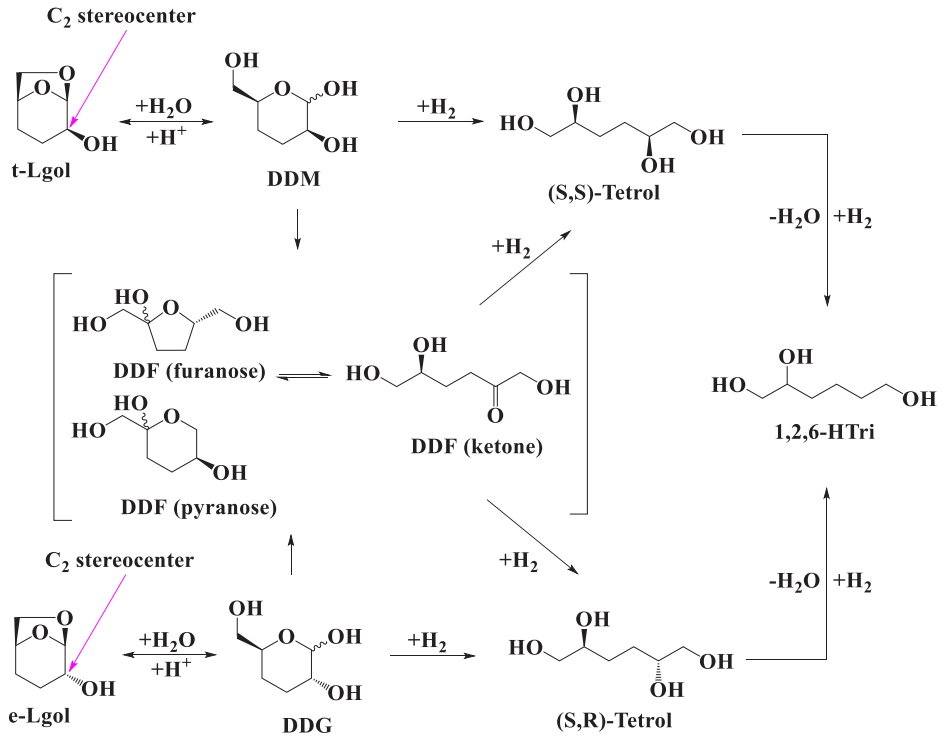

Figure 1. Lgol reaction network to tetrol[30] and HTri.[26] C_2 stereocenters of t-Lgol and e-Lgol and preserved (*S*,*S*) and (*S*,*R*) positions in tetrol shown.

cleavage of the anhydrobridge of Lgol in water over a Brønsted acid catalyst, forming the dideoxy sugar intermediates 3,4-dideoxymannose (DDM) from t-Lgol and 3,4-dideoxyglucose (DDG) from e-Lgol. The latter intermediates are then respectively hydrogenated over metal sites to (*S*,*S*)-tetrol and (*S*,*R*)-tetrol.[30] As an alternative pathway, it has also been established that DDM and DDG can isomerize to 3,4-dideoxyfructose (DDF) in the presence of a Lewis acid catalyst (at ≥100 °C) or at a somewhat elevated temperature (150 °C).[30] Subsequent hydrogenation of DDF leads to the formation of equal amounts of (*S*,*S*) and (*S*,*R*)-tetrol,[30] resulting in the complete loss of any of the initial Lgol stereochemistry on the C_2 stereocenter. We have previously shown that these reactions can be carried out selectively using bifunctional metal-acid catalysts, such as $Pt/SiO_2–Al_2O_3$, in which hydrolysis of Lgol to DDM and DDG occurs on acid sites, and subsequent hydrogenation of DDM, DDG, and DDF occurs on metal sites.[30] However, these reactions were done in a batch reactor where it is difficult to observe catalyst deactivation. In addition, while the selectivity to tetrol was 94%, this value was obtained at a reactant concentration of 2 wt % in water, with the value decreasing to 85% when a 20 wt % aqueous feed is used. It is desirable then to increase the reactant concentration and maintain high selectivity to tetrol with a stable and/or recyclable catalyst. A higher concentration of reactants and products is preferred industrially as it has lower downstream separation costs.[33] This is usually ignored in favor of low feed concentration (<5 wt %) tests that are easier to perform and understand on the laboratory scale.

Supported bifunctional catalysts have been shown very useful toward the hydrogenolysis of biomass-derived compounds.[10,25,27] These catalysts typically consist of a combination of reducible noble metals (e.g., Pt, Pd, Rh, Au), which engage in the adsorption and dissociation of H_2, and (reduced) oxophilic metal oxides (e.g., Mo, W, Re), which comprise the required acid sites capable of C–O cleavage reactions.[25,34−40] Such bifunctional catalysts are highly active in the hydrogenolysis of secondary C–O bonds of linear (particularly with –OH in nonprimary carbons) or cyclic polyoxygenates in which the carbon bonded to the oxygen or hydroxyl groups are vicinal due to the acid-catalyzed concerted formation of stable secondary oxocarbenium ion species in the former case, or primary oxocarbenium ion species stabilized with OH groups formed when the ring is protonated in the latter case,[25] which in both cases is then followed by metal-catalyzed hydrogenation. For example, Rh-ReO_x/C catalysts have been used in the hydrogenolysis of several cyclic polyoxygenates such as 2-(hydroxymethyl)tetrahydropyran (2-HMTHP) or tetrahydrofurfuryl alcohol to produce 1,6-HD and 1,5-pentanediol, respectively,[25,34] as well as the hydrogenolysis of fructose into HMF,[34] and of linear polyols such as butanediols and pentanediols.

Pt-WO_x/TiO_2 catalysts have been used previously by our group for hydrogenolysis reactions, such as THFDM conversion to 1,6-HD.[27] No correlation was found between the catalyst activity and any type of acid or metal site. We have previously proposed that the reaction occurs at the interface of the Pt and W, with the W^{5+} species possibly the active phase of the W. In this work, we carried out the selective hydrogenolysis of Lgol to form tetrol at high Lgol concentrations using Pt-WO_x/TiO_2 for the first time, measuring product selectivity with conversion, reaction kinetics (reaction orders and apparent activation energy) and catalyst stability with time-on-stream. We used a (10 wt %)Pt-(10 wt %)WO_x/TiO_2 catalyst composition because we have studied it for the conversion of THFDM hydrogenolysis to 1,6-HD, and this catalyst was shown to be the most active catalyst in terms of

https://doi.org/10.1021/acssuschemeng.1c04759
ACS Sustainable Chem. Eng. 2021, 9, 16123−16132

the rate of 1,6-HD production per total moles of Pt in the catalyst.

EXPERIMENTAL SECTION

Reagent Preparation. Lgol was prepared via quantitative hydrogenation of Cyrene (99%, Circa Group). Pure Cyrene was hydrogenated at 80 °C and 68.9 bar H_2 using 5 wt % Ru/C (Sigma-Aldrich) until complete conversion was achieved. The threo/erythro (t/e) ratio of the resulting Lgol was 1.8. The solid product Lgol was then extracted with acetone and filtered with a Buchner funnel with a fine fritted 80 mm diameter disc and then purified with the use of a rotoevaporator (Heidolph Hei-vap Advantage) at 60 °C to remove the majority of the acetone solvent. Afterward, the Lgol solution was further purified by transferring the contents of the rotoevaporator to falcon vials and putting them into a Speedvac (Savant Thermo Scientific) at room temperature.

Catalyst Synthesis. (10 wt %)Pt-(10 wt %)WO_x/TiO_2 catalysts (hereafter referred to as Pt-WO_x/TiO_2) were synthesized by wet impregnation of chloroplatinic acid on WO_x/TiO_2, which in turn was prepared from the method published by He et al.[27] A chloroplatinic acid solution in water was added to WO_x/TiO_2 support via wet impregnation. The mixture was then heated to 80 °C, while stirring; then, the resulting solid was dried at 80 °C in a vacuum oven overnight. The dry solid was then ground to a powder, and the powder was calcined under flowing air (Airgas, 19.5−23.5% O_2, 100 mL min^{-1}) at 400°C for 3 h (1°C min^{-1}) and subsequently reduced under flowing H_2 (Airgas, 99.999%, 100 mL min^{-1}) at 250°C for 2 h (1°C min^{-1}). After cooling down to room temperature, the catalysts were passivated under flowing 1% O_2 in Ar (Airgas, 99.999%) or transferred and stored in a glovebox.

Relevant catalyst characterization data for this work is reproduced from He et al.[27] and presented in Table S2 and Figures S4 and S5.

Batch Experiments. A 75 mL stainless steel Parr batch reactor with a dip-tube was used to carry out the batch experiments. Reactions were carried out with 40−45mL of reactant solution at 120°C, 600−1000 psi H_2 (99.999%, Airgas), 750 rpm stir rate and the desired amount of the powder catalyst. H_2 pressure was periodically replenished when the pressure fell to <90% of the desired value. Up to 6 samples were taken by first purging the dip-tube (0.3−0.5 mL) and then collecting the sample (0.5 mL/sample). A stainless-steel mesh was added to the dip-tube to retain the catalyst during sampling. Samples were diluted in water to obtain a 1−2 wt % solution that was then analyzed by HPLC. A BioRad Aminex 87H column was used in a Shimadzu HPLC. The mobile phase was 5 mM H_2SO_4 (HPLC grade, Ricca Chemical) operated at a flow rate of 0.6 mL min^{-1} with a column temperature of 30 °C and an injection volume of 3 μL. Lgol, HTri, DDM and tetrol plus intermediates DDG and DDF were quantified by HPLC using a refractive index (RI) detector. Lgol, tetrol and HTri response factors were obtained via calibration curves, whereas DDM, DDG, and DDF were assumed to be equal to tetrol. ^{13}C NMR was used to confirm the presence of Lgol, tetrol and HTri and quantify the stereoisomer ratios of Lgol and tetrol using a Bruker Avance-500 with a DCH cryoprobe. This information can be found in the Figure S1A−E. Details of HPLC chromatograms are also presented in the Figure S2A−D.

Conversion of Lgol is defined in the base of the reactant concentration as

$$X\ (\%) = \frac{C_{\mathrm{Lgol},0} - C_{\mathrm{Lgol}}}{C_{\mathrm{Lgol},0}} \tag{1}$$

Product selectivity is defined based on product concentration as

$$S_i\ (\%) = \frac{\frac{C_i}{C_{\mathrm{Lgol},0}}}{X\ (\%)} = \frac{Y_i\ (\%)}{X\ (\%)} \tag{2}$$

where Y_i (%) is the yield of the i-th product.

In the development of this work, the reactant conversion was fitted to a first-order kinetic model in the form of:

$$r_{\mathrm{Lgol}} = kC_{\mathrm{Lgol}} \tag{3}$$

where r_{Lgol} is in mmol g_{cat}^{-1} h^{-1}. From this, it follows that in a batch reactor, $C_{\mathrm{Lgol}}(t)$ is defined as

$$C_{\mathrm{Lgol}}(t) = C_{\mathrm{Lgol},0}\exp(-kt) \tag{4}$$

or alternatively as

$$\frac{C_{\mathrm{Lgol}}(t)}{C_{\mathrm{Lgol},0}} = \exp(-kt) \tag{5}$$

The activation energy derived from batch experiments is obtained from a linear fit of the Arrhenius equation defined as

$$E_a = -R\left[\frac{\partial \ln(r)}{\partial(1/T)}\right]_{P,C_i} \tag{6}$$

where E_{act} is the activation energy (kJ/mol), R is the universal gas constant (8.314 × 10^{-3} KJ mol^{-1} K^{-1}), T is temperature, and r is the initial rates of Lgol conversion obtained in the temperature range from 100 to 130 °C.

Flow Experiments. Lgol hydrogenolysis was carried out using a flow reactor to study its stability under time-on-stream (TOS). The reaction was carried out in a stainless-steel tubular flow reactor (2.0 in. length, 1/4 in. outer diameter), arranged in an up-flow configuration, and heated using a tube furnace (Applied Test Systems Inc. Series 3210). The catalyst (0.500 g) was sieved to 30−80 mesh sizes and added into the reactor with quartz wool packed on both sides without dilution. The material was reduced *in situ* under a H_2 flow (100 mL (STP) min^{-1}) at 250 °C for 2 h before reaction. The reactor was then heated to 120 °C and pressurized to 620 psi H_2, with pressure maintained using a back-pressure regulator. An aqueous 30 wt % Lgol solution was pumped into the reactor using a Teledyne Series I Legacy HPLC pump, with H_2 (40 mL (STP) min^{-1}) delivered by a mass flow controller (Brooks Instruments, 5850 Series E). A stainless-steel tank (150 mL) was used to accumulate the liquid products at the reactor outlet. The accumulated liquid product was collected periodically, filtered through a 0.22 μm PES syringe filter, diluted with water to 1−2 wt % concentration and then analyzed by HPLC. Feed solutions and liquid products were analyzed using HPLC as described for the batch experiments.

For first-order kinetics assuming ideal plug flow behavior, the Lgol conversion may be calculated as

$$X(\%) = 100 \times [1 - \exp(-k\tau)] \tag{7}$$

where τ is the space-time, which is defined in g_{cat} g_{Lgol}^{-1} h.

Catalyst and Product Characterization. Thermogravimetric analysis (TGA) of the spent and the fresh calcined materials was carried out using a TGA TA Q500. For analysis, 10−15 mg of a sample was added to the dish and heated up from room temperature to 650 °C at a 10 °C/min ramp under 50mL/min oxygen gas flow balanced with 50mL/min nitrogen gas flow.

Total organic carbon (TOC) analysis of the spent and the fresh catalyst was made with a Shimadzu TOC-V CPH/CPN using the SSM-5000A solid sample module under 100 mL/min oxygen flow. The instrument was calibrated with potassium phthalate (Acros Organics 417955000) from 0−80 mg, and 45−55 mg of sample was weighed for the analysis.

Pt, W, and Ti concentrations of the product effluents of the flow reactor were obtained by inductively coupled plasma optical emission spectroscopy (ICP-OES) with a Varian Vista-MPX after treating 1−1.5 g of the liquid samples with 1 wt % HNO_3 (trace metal grade, Sigma-Aldrich −438073) aqueous solution until pH < 1. Calibration curves of the metals were prepared from 1000 ppm standard solutions of Pt (Fluka, HONCE1046), W (Sigma-Aldrich, 50334), and Ti (Fluka, FLE1125). A similar ICP-OES analysis was done on the fresh calcined, spent, and recalcined catalyst samples using an Agilent 5110. Prior to measurement, ∼10 mg of a sample was digested in a mixture of 1 mL of HCl (Sigma-Aldrich no. 258148), 1 mL of HNO_3 (Sigma-

https://doi.org/10.1021/acssuschemeng.1c04759
ACS Sustainable Chem. Eng. 2021, 9, 16123−16132

Aldrich no. 438073), and 1 mL of HF (Sigma-Aldrich no. 339261) at 80 °C overnight.

Powder X-ray diffraction of the fresh calcined, spent, and recalcined catalyst samples was carried out in a Rigaku Rapid II diffractometer. A Mo Kα source (λ = 0.71 Å) was used for the measurements, and the scanned zone was 2θ = 5−60°. Structures were matched with the use of JADE, PDF 4+ software.

RESULTS AND DISCUSSION

Selectivity of Lgol Conversion in Water. *Selectivity to Different Products with Conversion.* Irrespective of the feed concentrations, the main observed products from Lgol conversion were tetrol and its three Lgol-derived intermediates DDM, DDG, and DDF. At higher conversions, HTri can also be detected. Figure 2 shows the product selectivity as a function of conversion for three different initial Lgol concentrations (10, 20, and 30 wt %). It can be observed that, at conversions in excess of 10%, tetrol and its DDM/DDG/DDF intermediates make up over 90% of the products. The nominal selectivity of products exceeds 100% for the 10 wt % Lgol feed due to tetrol, DDG, and DDF peaks fully overlapping (see Figure S2B), making quantitation difficult at low conversions as their individual response factors compound in that peak (note we assume DDM, DDG, and DDF response factors equal tetrol). HTri is present at conversions in excess of 40%, but its overall yield remains small (<3%, see Figure S2B−D). Furthermore, from quantitative ^{13}C NMR analysis (see Figure S1 and Table S1) of samples from the 20 wt %Lgol feed experiment, it could be concluded that HTri selectivity is constant with conversion, the values being 3.7% at 43% Lgol conversion and 3.5% at 91% Lgol conversion (see Table S1 for an average of peaks), and C-balances associated with these experiments can be found in Figure S6.

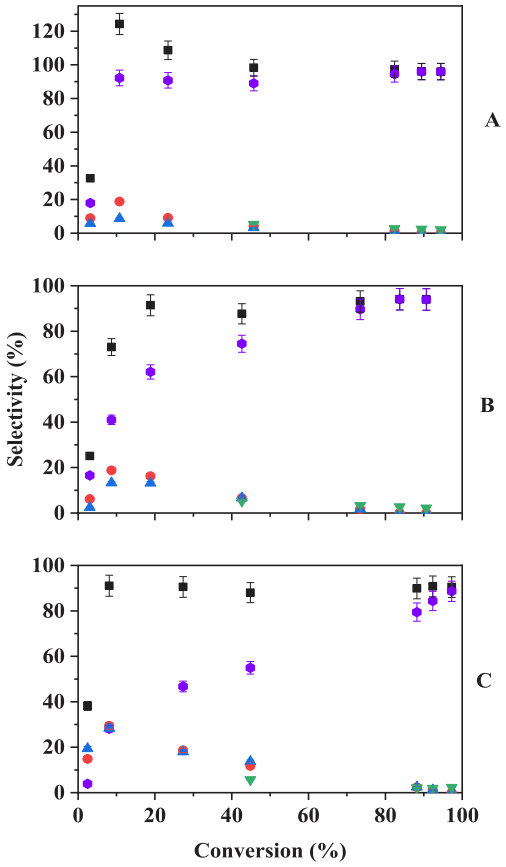

Figure 2. Calculated selectivities of tetrol + intermediates DDG/DDM/DDF (black squares), DDM (red circles), and HTri (green downward triangles) and estimated selectivities of tetrol (purple circles) and DDG (blue upward triangles) versus conversion using aqueous Lgol feed concentrations of (A) 10 wt %, (B) 20 wt %, and (C) 30 wt %. Conditions: 120 °C, 1000 psi H_2, 40−45 mL Lgol feed, 200 mg Pt-WO_x/TiO_2 catalyst.

To further understand the reaction network of the process, the selectivity of DDG was estimated (it is reminded that its peak and that of DDF overlaps completely with tetrol in HPLC analysis) by assuming that the ratio of produced DDM to DDG is proportional to the ratio of converted t-Lgol to converted e-Lgol and that negligible amounts of DDF are formed (as Lgol stereocenters were mostly preserved as will be shown later), while DDM is calculated normally with its own distinctive peak. Figure 2 shows the resulting selectivity trends for DDM, the estimated DDG, and the estimated tetrol selectivity obtained after subtracting DDG from the total selectivity of the tetrol + DDG + DDF peak (with DDF → 0). It can be observed that tetrol now appears as a secondary stable product, whereas DDM and DDG appear as unstable products, reflecting their conversion to tetrol in a series mechanism, which is consistent with previous work done by our group on the reaction network of Lgol conversion to tetrol with Pt/SiO_2−Al_2O_3.[30] Regarding HTri, it can be asserted that it is a stable product since the measured selectivity is relatively constant with conversion. Moreover, since it can only be observed at >40% conversion, it cannot be asserted to what degree HTri may come from tetrol (or not) since concentrations before this conversion may just be below detection limits for HPLC and NMR. These results already constitute an improvement from our prior work[30] since we are able to obtain >90% selectivity to tetrol with feeds as concentrated as 30 wt %. With Pt/SiO_2−Al_2O_3 tetrol, selectivity was 85% when a 20 wt % aqueous Lgol feed is used. Pt-WO_x/TiO_2 is able to selectivity produce tetrol from Lgol.[28,29]

Neither THFDM nor its isomer tetrahydropyran-2-methanol-5-hydroxyl (THP2M5H) was observed (refer to Figure S1A−E). This is in contrast with prior work done by our group on the Pt/SiO_2−Al_2O_3-catalyzed Lgol to tetrol conversion.[30] It has been previously shown that THFDM can be produced as a main product from Lgol hydrogenolysis in organic solvent[23] or as a minor byproduct in aqueous media.[30] THFDM has also been reported as a product of acid-catalyzed tetrol dehydration[20] and can also convert to HTri in a series mechanism.[24] Pt-WO_x/TiO_2 and similar catalysts are known to catalyze C−O bond hydrogenolysis reactions of other oxygenated molecules, such as THFDM and HTri.[24,26,27] The selectivity to HTri is very low (1−6%), indicating that the rate of tetrol to HTri is much lower than that of Lgol to tetrol. This is consistent with previously reported higher reaction rates of −OH-substituted cyclic ethers to linear polyols compared to the rate of more substituted linear polyol to less substituted ones using similar catalysts. For instance, the reaction rate of 2-HMTHP to 1,6-HD (90 μmol g min^{-1}) is higher than HTri conversion to 1,6-HD (23 μmol g min^{-1}), which in turn is greater than the rate of conversion of 1,6-HD to 1-hexanol (no visible reaction) at 100 °C using $RhReO_x$/C as reported by Chia et al.[25]

Stereochemistry of Lgol Conversion to Tetrol with Pt-WO_x/TiO_2. We previously showed that the obtained Lgol t/e

https://doi.org/10.1021/acssuschemeng.1c04759
ACS Sustainable Chem. Eng. 2021, 9, 16123−16132

ratio depends on the choice of the catalyst used to hydrogenate Cyrene.[22] As shown in Figure 1, the C_2−OH stereocenter can either be preserved or erased depending on whether the intermediates DDM and DDG are rapidly hydrogenated to (*S*,*S*)- and (*S*,*R*)-tetrol or isomerized to DDF prior to hydrogenation.[30] In this work, we used Lgol with a feedstock t/e ratio of 1.8 and obtained a tetrol (*S*,*S*)/(*S*,*R*) ratio of 1.7 at 91% Lgol conversion over a Pt-WO_x/TiO_2 catalyst (T = 120 °C). This corresponds to 91% preservation of the diastereomeric excess present in the Lgol feedstock. In contrast, a maximum of 64% preservation of diastereomeric excess in Lgol was obtained over a 5% Pt/SiO_2−Al_2O_3 catalyst at near-complete Lgol conversion (T = 150 °C).[30] A lower temperature (T = 100 °C) two-step route using hydrolysis over an Amberlyst 70 acid catalyst, followed by hydrogenation over 5% Pt/SiO_2, was able to largely preserve the Lgol stereochemistry (92%). However, in the latter case, the initial Lgol hydrolysis step is equilibrium-limited, thus only allowing for a maximum t- and e-Lgol conversion of 58 and 83%, respectively.[30] In this work, we achieved a high degree of stereochemistry preservation at near-complete Lgol conversion because (i) the rate of aldose-ketose isomerization that scrambles the C_2−OH stereocenter (observed in our previous work at 150 °C)[23,30] is very low at 120 °C and (ii) the bifunctional metal-acid catalyst hydrogenates DDM and DDG *in situ* at a higher rate than isomerization to DDF (evidenced by the absence of intermediates at ∼90% conversion), enabling complete Lgol conversion.

Kinetic Parameter Measurements. *Reaction Orders of Lgol and H_2.* Reaction orders and the apparent activation energy for Lgol conversion were measured in a batch reactor using 10, 20, and 30 wt % aqueous Lgol solutions and a fixed pressure of 1000 psi H_2. Figure 3 shows the normalized

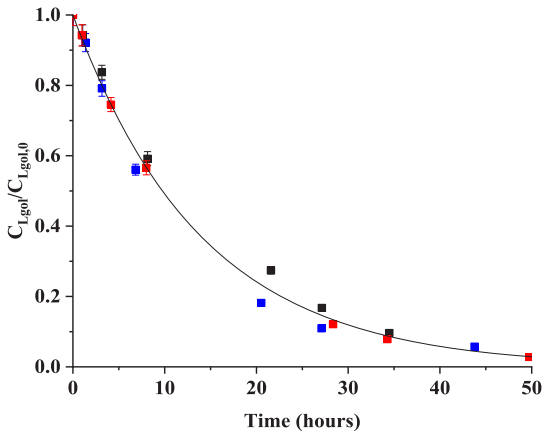

Figure 3. Normalized Lgol concentration vs time in batch reactor and first-order fit for Lgol hydrogenolysis in water with Lgol concentration feeds of 10 wt % (blue squares), 20 wt % (black squares), and 30 wt % (red squares) using the Pt-WO_x/TiO_2 catalyst. The black line is Lgol first-order function fit described by eq 5, where k = 0.071 ± 0.004, adjusted R^2 = 0.9951. Conditions: 120 °C, 1000 psi H_2, 40−45 mL Lgol feed, 200 mg of catalyst.

reactant concentration versus time and the resulting first-order model fit for the whole data set done with eq 5. The value obtained for the first-order rate constant k is 0.071 ± 0.004 h^{-1} (95% confidence interval-based, as are all function fits hereafter). This value is consistent with one calculated from the product concentration (see Figure S3), which has a larger error of 0.006 h^{-1} due to the overlap of several of the products (tetrol and intermediates) at lower conversions (<20%) compared to higher ones (∼40%). The maximum total number of turnovers for the batch reactions were 1570 $mmol/mmol_{acid}$ and 5650 $mmol/mmol_{Pt}$ (surface sites). Three experiments were carried out at 600, 800, or 1000 psi H_2 and 20 wt % Lgol to measure the reaction order with respect to H_2. As shown in Figure 4, the reaction is zero-order in H_2.

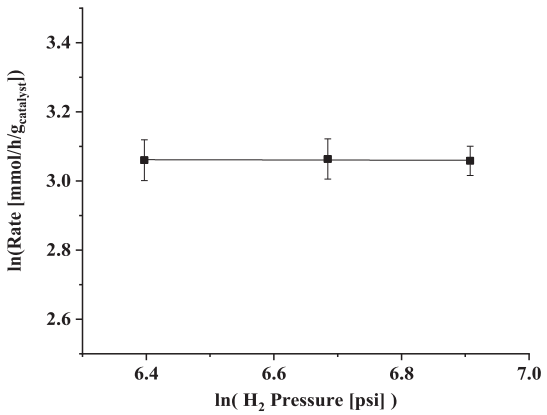

Figure 4. Hydrogen reaction order (n_{H_2}) plot for Lgol hydrogenolysis in water in a batch reactor using the Pt-WO_x/TiO_2 catalyst. n_{H_2} = 0.00 ± 0.02. Conditions: 120 °C, 35−40 mL aqueous 20 wt % Lgol feed, 175−200 mg of catalyst, 600, 800, or 1000 psi H_2.

The reaction orders obtained for this work are similar to those obtained by Krishna et al.[23] for Lgol conversion in a polar aprotic solvent (THF), where the major product (THFDM) is formed via irreversible, rate-limiting acid-catalyzed C−O bond cleavage followed by metal-catalyzed hydrogenation to THFDM.[23] The reaction orders obtained in this work fit the interpretation of an irreversible acid-catalyzed C−O bond cleavage step followed by hydrogenation on a metal site. If acid-catalyzed Lgol hydrolysis were reversible, a positive H_2 dependence might be expected because hydrogenation would promote the rate of Lgol hydrolysis by shifting the equilibrium to the products of that reaction step. However, it is also possible that the zeroth reaction order for H_2 is a consequence of metal sites being saturated by H_2. More studies in which the Pt loading of the catalyst is varied are necessary to fully ascertain the impact of the hydrogenation rate compared to the acid-catalyzed reaction rate.

Activation Energy for Lgol Conversion in Water. The apparent activation energy of Lgol hydrogenolysis in water was calculated by performing experiments at 100−130 °C with 20 wt % Lgol aqueous feeds. The apparent activation energy was found to be 151 ± 10 kJ/mol, as shown in Figure 5. This apparent activation energy value is higher than those reported in literature for hydrogenolysis of C−O bonds of cyclic ethers[25] (84−118 kJ/mol) and also higher than the computed activation energy of Lgol hydrolysis with H_2SO_4 catalyst (t-Lgol to DDM: 86 kJ/mol; e-Lgol to DDG: 98 kJ/mol) in water.[41]

Catalyst Performance and Stability and Activity in a Flow Reactor. Figure 6 shows the performance of the Pt-WO_x/TiO_2 catalyst for the hydrogenolysis of a 30 wt % aqueous Lgol solution at 120 °C over 51 h time-on-stream (TOS). The number of turnovers for this catalyst during the time period (∼51 h) based on surface metal and acid sites are

https://doi.org/10.1021/acssuschemeng.1c04759
ACS Sustainable Chem. Eng. 2021, 9, 16123−16132

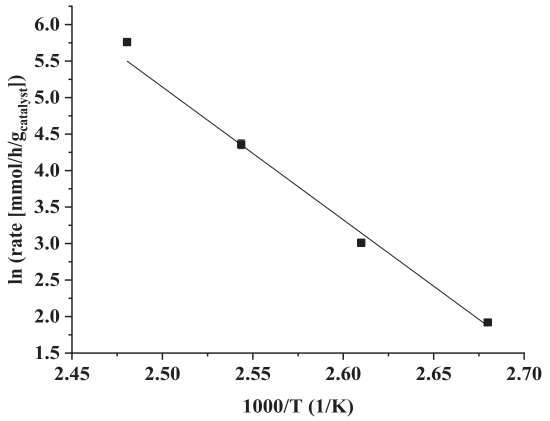

Figure 5. Activation energy plot for Lgol hydrogenolysis in water using the Pt-WO_x/TiO_2 catalyst done with eq 6. E_{app} = 151 ± 10 kJ/mol, adjusted R^2 = 0.9904. Reaction conditions: 1000 psi H_2, 40 mL aqueous 20 wt % Lgol feed, 50−200 mg catalyst, 100, 110, 120, or 130 °C.

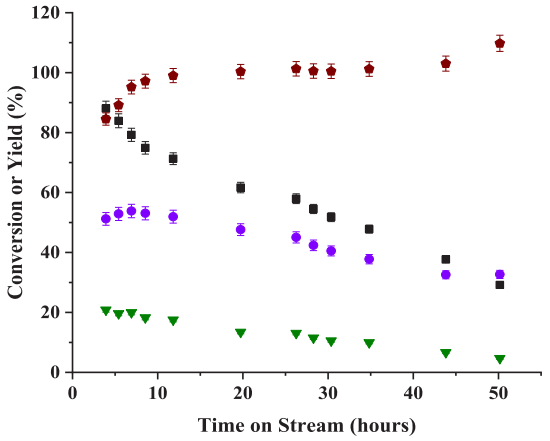

Figure 6. Conversion (black squares), yields of tetrol + intermediates (purple circles) and HTri (green triangles), and carbon balances (brown pentagons) vs time on stream for Lgol hydrogenolysis in a flow reactor using the Pt-WO_x/TiO_2 catalyst. Reaction conditions: 30 wt % aqueous Lgol feed, 120 °C, 620 psi H_2, 500 mg of catalyst, 20 μL/min liquid flow, 40 mL/min H_2 flow.

1435 mmol/mmol$_{Pt}$ (CO chemisorption) and 400 mmol/mmol$_{acid}$ (NH_3-TPD), respectively. The catalyst was deactivated with TOS. The catalyst was found to produce tetrol and its intermediates (DDM, DDG, and DDF) initially in yields over 50% for conversions greater than 80%. HTri was also detected in the products, with yields being over 20% at initial times.

The tetrol selectivity, its intermediates, and HTri selectivity are analyzed at the different conversions measured over time in Figure 7. The tetrol selectivity decreases as conversion increases. The HTri selectivity increases slightly with conversion from 16% at 29% conversion to 23% at 88% conversion. The HTri selectivity in the continuous flow reactor is higher than the values obtained for batch experiments (1−6%). The calculated conversion in a flow reactor using the rate constant value obtained from the batch (0.071 h^{-1}) at the weight hourly space velocity set in the flow reaction experiment (0.605 g_{Lgol} g_{cat} h^{-1}) using eq 7 is 100%, and the initial conversion estimated at $t \rightarrow 0$ from Figure 7 is over 90%, showing a slight difference between both reactors in regards

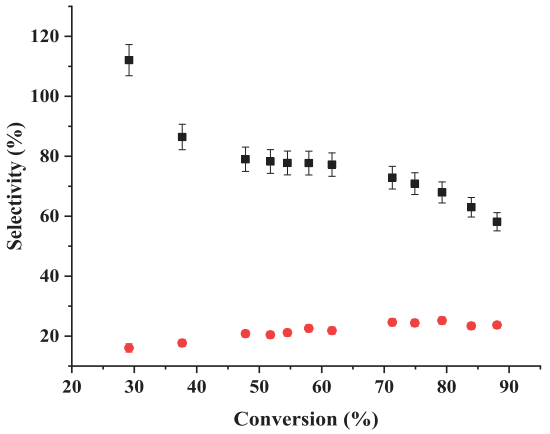

Figure 7. Selectivity of detected products tetrol + intermediates (black squares) and HTri (red circles) vs conversion for Lgol hydrogenolysis in a flow reactor using the Pt-WO_x/TiO_2 catalyst. Conditions as described in Figure 6.

Lgol consumption. Therefore, we hypothesize that the difference in HTri selectivity between batch and flow experiments is because of deviations of ideal plug-flow reactor behavior that arise from (i) catalyst deactivation and (ii) complex hydrodynamic effects that may arise by having a two-phase liquid and gas flow that, in turn, can affect product selectivity at a given conversion when compared to a batch reactor. A detailed hydrodynamic analysis of this two-phase continuous flow reactor is beyond the scope of this paper. However, an example of such complex effects can be observed in the aqueous-phase hydrogenation of acetic acid using Ru catalysts, in which methane is the main product when the reaction is carried out in a batch reactor,[42] and ethanol is the main product in this reaction when the hydrogenation is done in a two-phase continuous flow reactor.[43]

Often in biomass catalytic conversion reactions, increased reactant concentrations lead to lower selectivity to monomeric products due to oligomerization reactions that form undesired degradation products ("humins").[44,45] In this work, product samples were dark brown, suggesting the formation of oligomeric humins. However, carbon balances (100%[1 − C_{out}/C_{in}]) were 98% on average, indicating that selectivity was mostly to detectable products. The full C-balance profile over time on stream can be observed in Figure 6. At initial data points (<10 h TOS), C-balances were on the lower side, indicating potential carbon loss to undetectable products. At the last data point (51 h TOS), C-balance shows an accumulation of ∼10% carbon compared to the initial source, which may occur due to water evaporation.

The spent catalyst was calcined at 450 °C for 4 h (1 °C/min) and rereduced at 250 °C for 2 h (1 °C/min), and the continuous flow reaction experiment was subsequently repeated. The result is shown in Figure S7. The catalyst regained some of its reactivity, but its initial conversion was 51%, being lower than the fresh catalyst (88%). Therefore, the catalyst was concluded to be only partially regenerable.

We measured the concentrations of Pt and W in the product effluent.[26] W was found to leach into the product effluent, while no Pt leaching was detected. The results of W-leaching for the first flow reaction run are shown in Figure 8. The concentration of leached W decreased with time on stream. The total amount of W-leached in the continuous flow experiment with the fresh catalyst corresponding to 3.7% of the

https://doi.org/10.1021/acssuschemeng.1c04759
ACS Sustainable Chem. Eng. 2021, 9, 16123−16132

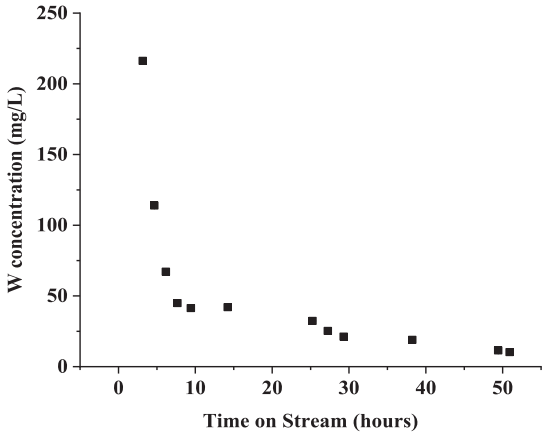

Figure 8. W-leached detected in products as a function of time on stream in the first run with Pt-WO_x/TiO_2 over 51 h. Conditions as described in Figure 6.

total W mass of the fresh catalyst. W-leaching during the second run (following catalyst regeneration) is shown in Figure S8. The W-leaching rate is similar to that at the end of the first run, suggesting that the W-leaching rate decreases and even stabilizes as more of the metal is lost to the product solution. This trend was also observed by our group in a prior work.[26] ICP-OES was also performed on the fresh and spent catalyst. We found a small decrease in both Pt and W content compared to the fresh as shown in Table S3. The catalyst initially lost W and maybe Pt, which would be consistent with loss of activity with time on stream. The number of acid sites, as measured by NH_3-TPD, of the fresh and spent catalyst was essentially the same. This is consistent with our previous work,[27] which shows that the acid sites do not correlate with catalyst activity. Powder XRD analysis of the fresh, spent, and recalcined samples presented in Figure S9 shows no significant change in the crystalline structure of the catalyst after reaction and regeneration.

TGA and TOC analyses on the spent catalyst samples were used to determine the amount of carbon deposited on the catalyst during continuous flow experiments. Figure 9 contains the weight loss profile of the spent sample compared to the fresh observed in the TGA analyses. Two peaks at around 200 and 225 °C were observed. The TOC analysis showed that 11% of the catalyst mass was carbon compared to 2% of the fresh catalyst. The TOC results roughly match the weight loss showed between the two peaks attributed to carbon between 150−250 °C by TGA. The wide peak that occurs at about 120 °C then can be attributed mostly to water adsorbed in the catalyst from the reactant feed and the environment. The fresh calcined catalyst shows no significant mass loss over time (∼1.5%). These results indicate that carbonaceous species are deposited on the catalyst surface during the reaction and could thus contribute to catalyst deactivation. These species are removed by the regeneration treatment used here (450 °C calcination followed by a reduction *in situ* at 250 °C). Deposition of carbonaceous species could contribute to catalyst deactivation but cannot explain the irreversible loss of reactivity despite regeneration treatments.

It is therefore noted that the different deactivation mechanisms at play may affect product selectivity and result in the discrepancies between batch and flow reactor results, especially if the rate at which each type of active site is deactivated differs significantly. Leaching, for instance, has the potential to be more pervasive for flow experiments than from batch due to W being completely lost in the liquid stream, whereas, in the batch, it may still remain active in solution. We remind that W loading and its oxidation state affect activity.[27] Also, intrinsic differences in the way H_2 is added between batch and flow reactors and initial conversion differences between the two of them may also affect the rate of coking of the catalyst, since it is noted that, in batch experiments, the reaction was able to be run at near-complete conversions for different Lgol feeds, requiring more turnovers for this than reported for the continuous flow experiment (up to 1570 $mmol/mmol_{acid}$ in the batch vs 400 $mmol/mmol_{acid}$ in the flow reactor as shown in Figure 10). However, note that there is no direct correlation between acid or metal sites and activity[27] and that, only when this correlation is found, a more direct comparison of turnovers between batch and flow will be possible.

Finally, a (5 wt %) Pt/SiO_2−Al_2O_3 catalyst was studied for Lgol hydrogenolysis with a 2 wt % aqueous Lgol at 150 °C. Figure 10 shows the number of turnovers (in surface acid sites) for Pt/SiO_2−Al_2O_3 and Pt-WO_x/TiO_2. The Pt-WO_x/TiO_2 is more stable and active than the Pt/SiO_2−Al_2O_3. Figure S10 shows the conversion vs time on stream profile for 5 wt %Pt/SiO_2−Al_2O_3, and it can be observed that the catalyst deactivates over 45 h TOS. Treatment of the spent Pt/SiO_2−Al_2O_3 catalyst via calcination in air at 400 °C and reduction at 260 °C for 1 h did not regenerate the catalytic reactivity (5% initial conversion was measured in a subsequent

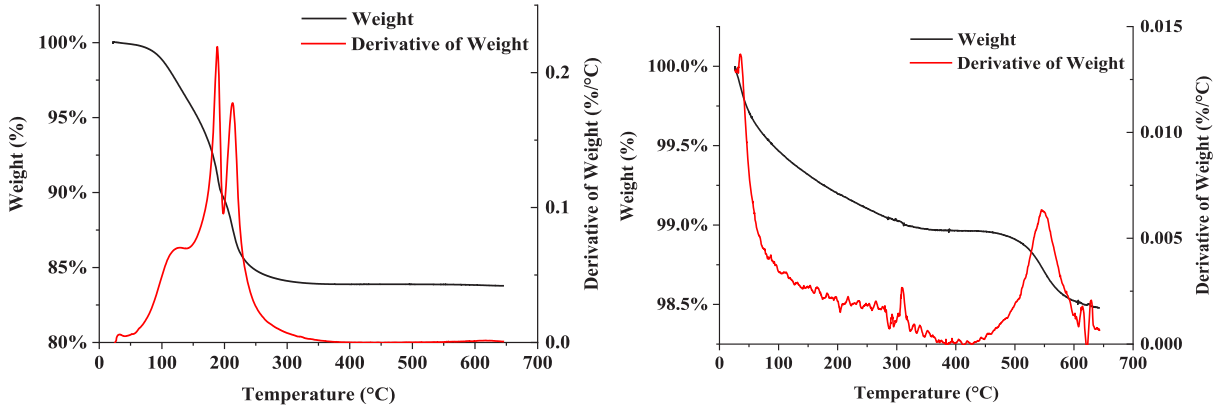

Figure 9. TGA weight loss profile for the Pt-WO_x/TiO_2 spent (left) and fresh (right) catalyst.

https://doi.org/10.1021/acssuschemeng.1c04759
ACS Sustainable Chem. Eng. 2021, 9, 16123−16132

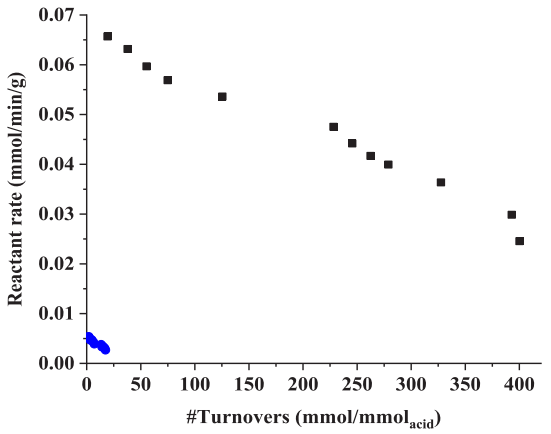

Figure 10. Reactant rates with a number of turnovers (surface acid site basis) for Pt-WO_x/TiO_2 (black squares) and $Pt/SiO_2-Al_2O_3$ (blue circles) catalysts. Conditions: For Pt-WO_x/TiO_2 as described in Figure 6. For $Pt/SiO_2-Al_2O_3$: 2 wt % aqueous Lgol feed, 130 °C, 500 psi H_2, 200 mg of catalyst, 30 μL/min feed flow, 6 mL/min H_2 flow.

continuous flow experiment). Amorphous silica−aluminas are known to undergo irreversible deactivation in water at high temperatures.[45,46] From this performance comparison and the information presented in this study, it can be reasonably argued that 10 wt %Pt-10 wt %WO_x/TiO_2 can be used at lower temperatures and still retain significant activity. Future work in this area could study how to reduce the Pt loading of the catalyst since the H_2 reaction order for Lgol hydrogenolysis to tetrol is zero. In addition, it may be possible to use a lower-cost metal such as Ni or Cu for the hydrogenation step. The stability and recyclability of the best such catalysts may also be further studied in-depth.

CONCLUSIONS

Hydrogenolysis of Lgol was carried out in water under high reactant concentrations (i.e., 10−30 wt %) using (10 wt %)Pt-(10 wt %)WO_x/TiO_2 catalyst. The catalyst is highly selective to tetrol and its intermediates (e.g., >90% selectivity at >20% conversion in a batch reactor). The catalyst showed deactivation but is more stable than a 5 wt %$Pt/SiO_2-Al_2O_3$. The catalyst activity can be partially recovered by a rereduction/oxidation treatment. The reaction is first order with respect to Lgol and zero order with respect to H_2. The observed kinetics are consistent with irreversible acid-catalyzed C−O bond cleavage of Lgol to form intermediates that are then hydrogenated to tetrol. This route largely preserves the stereocenters in the Lgol feedstock, converting t-Lgol to (*S*,*S*)-tetrol and e-Lgol to (*S*,*R*)-tetrol with 91% overall preservation of the C_2 stereocenters. Stereocenter preservation implies that reactive aldose intermediates (DDM, DDG) formed over acid sites are rapidly hydrogenated over metal sites at rates much higher than their isomerization to ketose (DDF) intermediates that erase the C_2 stereocenter.

ASSOCIATED CONTENT

Supporting Information

The Supporting Information is available free of charge at https://pubs.acs.org/doi/10.1021/acssuschemeng.1c04759.

^{13}C-qNMR spectra and peak information; relevant information for HPLC peak identification and deconvolution; reactant vs product fit comparison for first-order Lgol fit; relevant catalyst characterization data; carbon balance information for batch experiments; catalyst reuse after regeneration data and spent catalyst relevant characterization data; conversion vs TOS for 5 wt %Pt/SiO_2-AlO_3 data (PDF)

AUTHOR INFORMATION

Corresponding Author

George W. Huber − *Department of Chemical and Biological Engineering, University of Wisconsin−Madison, Madison, Wisconsin 53706, United States;* orcid.org/0000-0002-7838-6893; Email: gwhuber@wisc.edu

Authors

Paolo Cuello-Penaloza − *Department of Chemical and Biological Engineering, University of Wisconsin−Madison, Madison, Wisconsin 53706, United States*

Siddarth H. Krishna − *Department of Chemical and Biological Engineering, University of Wisconsin−Madison, Madison, Wisconsin 53706, United States*

Mario De bruyn − *Department of Chemical and Biological Engineering, University of Wisconsin−Madison, Madison, Wisconsin 53706, United States; Faculty of Science, Debye Institute for Nanomaterials Science, Utrecht University, 3584 CG Utrecht, The Netherlands; Institute for Chemistry, Organic and Bioorganic Chemistry, University of Graz, 8010 Graz, Austria;* orcid.org/0000-0002-9687-1606

Bert M. Weckhuysen − *Faculty of Science, Debye Institute for Nanomaterials Science, Utrecht University, 3584 CG Utrecht, The Netherlands;* orcid.org/0000-0001-5245-1426

Edgard A. Lebrón-Rodríguez − *Department of Chemistry, University of Wisconsin−Madison, Madison, Wisconsin 53706, United States*

Ive Hermans − *Department of Chemistry, University of Wisconsin−Madison, Madison, Wisconsin 53706, United States;* orcid.org/0000-0001-6228-9928

James A. Dumesic − *Department of Chemical and Biological Engineering, University of Wisconsin−Madison, Madison, Wisconsin 53706, United States;* orcid.org/0000-0001-6542-0856

Complete contact information is available at: https://pubs.acs.org/10.1021/acssuschemeng.1c04759

Notes

The authors declare no competing financial interest.

ACKNOWLEDGMENTS

We thank the University of Wisconsin−Madison, Department of Chemistry, for the use of the Bruker Avance 500 MHz NMR spectrometer. A generous gift from Paul J. Bender enabled this spectrometer to be purchased. We also thank Circa Group for generously supplying Cyrene, from which we synthesized the levoglucosanol used in this work. S.H.K. acknowledges that this material is based upon work supported by the National Science Foundation (DGE-1256259).

REFERENCES

(1) Krishna, S. H.; Walker, T. W.; Dumesic, J. A.; Huber, G. W. Kinetics of Levoglucosenone Isomerization. *ChemSusChem* **2017**, *10* (1), 129−138.

(2) Flourat, A. L.; Peru, A. A. M.; Teixeira, A. R. S.; Brunissen, F.; Allais, F. Chemo-Enzymatic Synthesis of Key Intermediates (S)-γ-Hydroxymethyl-α,β-Butenolide and (S)-γ-Hydroxymethyl-γ-Butyro-

lactone via Lipase-Mediated Baeyer−Villiger Oxidation of Levoglucosenone. *Green Chem.* **2015**, *17* (1), 404−412.
(3) Stockton, K. P.; Greatrex, B. W. Synthesis of Enantiopure Cyclopropyl Esters from (−)-Levoglucosenone. *Org. Biomol. Chem.* **2016**, *14* (31), 7520−7528.
(4) Giri, G. F.; Danielli, M.; Marinelli, R. A.; Spanevello, R. A. Cytotoxic Effect of Levoglucosenone and Related Derivatives against Human Hepatocarcinoma Cell Lines. *Bioorg. Med. Chem. Lett.* **2016**, *26* (16), 3955−3957.
(5) Giri, G. F.; Viarengo, G.; Furlán, R. L. E.; Suárez, A. G.; Garcia Véscovi, E.; Spanevello, R. A. Soybean Hulls, an Alternative Source of Bioactive Compounds: Combining Pyrolysis with Bioguided Fractionation. *Ind. Crops Prod.* **2017**, *105*, 113−123.
(6) Shafizadeh, F.; Furneaux, R. H.; Stevenson, T. T. Some Reactions of Levoglucosenone. *Carbohydr. Res.* **1979**, *71* (1), 169−191.
(7) Sherwood, J.; De bruyn, M.; Constantinou, A.; Moity, L.; McElroy, C. R.; Farmer, T. J.; Duncan, T.; Raverty, W.; Hunt, A. J.; Clark, J. H. Dihydrolevoglucosenone (Cyrene) as a Bio-Based Alternative for Dipolar Aprotic Solvents. *Chem. Commun.* **2014**, *50* (68), 9650−9652.
(8) De bruyn, M.; Cuello-Penaloza, P.; Cendejas, M.; Hermans, I.; He, J.; Krishna, S. H.; Lynn, D. M.; Dumesic, J. A.; Huber, G. W.; Weckhuysen, B. M. Hexane-1,2,5,6-Tetrol as a Versatile and Biobased Building Block for the Synthesis of Sustainable (Chiral) Crystalline Mesoporous Polyboronates. *ACS Sustainable Chem. Eng.* **2019**, *7* (15), 13430−13436.
(9) Wilson, K. L.; Kennedy, A. R.; Murray, J.; Greatrex, B.; Jamieson, C.; Watson, A. J. B. Scope and Limitations of a DMF Bio-Alternative within Sonogashira Cross-Coupling and Cacchi-Type Annulation. *Beilstein J. Org. Chem.* **2016**, *12*, 2005−2011.
(10) Tamura, M.; Nakagawa, Y.; Tomishige, K. Reduction of Sugar Derivatives to Valuable Chemicals: Utilization of Asymmetric Carbons. *Catal. Sci. Technol.* **2020**, *10* (12), 3805−3824.
(11) Krishna, S. H.; Cao, J.; Tamura, M.; Nakagawa, Y.; De Bruyn, M.; Jacobson, G. S.; Weckhuysen, B. M.; Dumesic, J. A.; Tomishige, K.; Huber, G. W. Synthesis of Hexane-Tetrols and -Triols with Fixed Hydroxyl Group Positions and Stereochemistry from Methyl Glycosides over Supported Metal Catalysts. *ACS Sustainable Chem. Eng.* **2020**, *8* (2), 800−805.
(12) Warmington, A. Consortium to build Cyrene plant. https://www.specchemonline.com/consortium-build-cyrene-plant (accessed 05/12/2020).
(13) Flagship EU Project aiming to Replace Toxic Solvents with Renewable Alternatives Launches Today. https://circa-group.com/news/2020/10/24/9axo6z01ddll227lq24abjs2g5mbyz (accessed 03/24/2021).
(14) De Bruyn, M.; Fan, J.; Budarin, V. L.; Macquarrie, D. J.; Gomez, L. D.; Simister, R.; Farmer, T. J.; Raverty, W. D.; McQueen-Mason, S. J.; Clark, J. H. A New Perspective in Bio-Refining: Levoglucosenone and Cleaner Lignin from Waste Biorefinery Hydrolysis Lignin by Selective Conversion of Residual Saccharides. *Energy Environ. Sci.* **2016**, *9* (8), 2571−2574.
(15) Stock announcements. https://circa-group.com/stock-announcements (accessed 6/11/2021).
(16) Cao, F.; Schwartz, T. J.; McClelland, D. J.; Krishna, S. H.; Dumesic, J. A.; Huber, G. W. Dehydration of Cellulose to Levoglucosenone Using Polar Aprotic Solvents. *Energy Environ. Sci.* **2015**, *8* (6), 1808−1815.
(17) Mazarío, J.; Romero, M. P.; Concepción, P.; Chávez-Sifontes, M.; Spanevello, R. A.; Comba, M. B.; Suárez, A. G.; Domine, M. E. Tuning Zirconia-Supported Metal Catalysts for Selective One-Step Hydrogenation of Levoglucosenone. *Green Chem.* **2019**, *21* (17), 4769−4785.
(18) Milescu, R. A.; Zhenova, A.; Vastano, M.; Gammons, R.; Lin, S.; Lau, C. H.; Clark, J. H.; McElroy, C. R.; Pellis, A. Polymer Chemistry Applications of Cyrene and Its Derivative Cygnet 0.0 as Safer Replacements for Polar Aprotic Solvents. *ChemSusChem* **2021**, *14* (16), 3367−3381.
(19) Adaka, I. C.; Uzor, P. F. Chapter 12 - Cyrene as a Green Solvent in the Pharmaceutical Industry. *Green Sustainable Process for Chemical and Environmental Engineering and Science* **2021**, 243−248.
(20) De bruyn, M.; Budarin, V. L.; Misefari, A.; Shimizu, S.; Fish, H.; Cockett, M.; Hunt, A. J.; Hofstetter, H.; Weckhuysen, B. M.; Clark, J. H.; Macquarrie, D. J. Geminal Diol of Dihydrolevoglucosenone as a Switchable Hydrotrope: A Continuum of Green Nanostructured Solvents. *ACS Sustainable Chem. Eng.* **2019**, *7* (8), 7878−7883.
(21) De bruyn, M.; Sener, C.; Petrolini, D. D.; McClelland, D. J.; He, J.; Ball, M. R.; Liu, Y.; Martins, L.; Dumesic, J. A.; Huber, G. W.; Weckhuysen, B. M. Catalytic Hydrogenation of Dihydrolevoglucosenone to Levoglucosanol with a Hydrotalcite/Mixed Oxide Copper Catalyst. *Green Chem.* **2019**, *21* (18), 5000−5007.
(22) Krishna, S. H.; McClelland, D. J.; Rashke, Q. A.; Dumesic, J. A.; Huber, G. W. Hydrogenation of Levoglucosenone to Renewable Chemicals. *Green Chem.* **2017**, *19* (5), 1278−1285.
(23) Krishna, S. H.; Assary, R. S.; Rashke, Q. A.; Schmidt, Z. R.; Curtiss, L. A.; Dumesic, J. A.; Huber, G. W. Mechanistic Insights into the Hydrogenolysis of Levoglucosanol over Bifunctional Platinum Silica−Alumina Catalysts. *ACS Catal.* **2018**, *8* (5), 3743−3753.
(24) Buntara, T.; Melián-Cabrera, I.; Tan, Q.; Fierro, J. L. G.; Neurock, M.; Vries, J. G. D.; Heeres, H. J. Catalyst Studies on the Ring Opening of Tetrahydrofuran-Dimethanol to 1,2,6-Hexanetriol. *Catal. Today* **2013**, *210*, 106−116.
(25) Chia, M.; Pagán-Torres, Y. J.; Hibbitts, D.; Tan, Q.; Pham, H. N.; Datye, A. K.; Neurock, M.; Davis, R. J.; Dumesic, J. A. Selective Hydrogenolysis of Polyols and Cyclic Ethers over Bifunctional Surface Sites on Rhodium−Rhenium Catalysts. *J. Am. Chem. Soc.* **2011**, *133* (32), 12675−12689.
(26) He, J.; Burt, S. P.; Ball, M. R.; Hermans, I.; Dumesic, J. A.; Huber, G. W. Catalytic C-O Bond Hydrogenolysis of Tetrahydrofuran-Dimethanol over Metal Supported WOx/TiO2 Catalysts. *Appl. Catal., B* **2019**, *258*, 117945.
(27) He, J.; Burt, S. P.; Ball, M.; Zhao, D.; Hermans, I.; Dumesic, J. A.; Huber, G. W. Synthesis of 1,6-Hexanediol from Cellulose Derived Tetrahydrofuran-Dimethanol with Pt-WO_x /TiO $_2$ Catalysts. *ACS Catal.* **2018**, *8* (2), 1427−1439.
(28) Allgeier, A. M.; Ritter, J. C.; Sengupta, S. K., Process for Preparing 1,6-Hexanediol. US20130231505, September 5, 2013.
(29) Allgeier, A. M.; De Silva, W. I. N.; Korovessi, E.; Menning, C. A.; Ritter, J. C.; Sengupta, S. K.; Stauffer, C. S. Process for Preparing 1,6-Hexanediol. US8865940B2, October 21, 2014.
(30) Krishna, S. H.; De bruyn, M.; Schmidt, Z. R.; Weckhuysen, B. M.; Dumesic, J. A.; Huber, G. W. Catalytic Production of Hexane-1,2,5,6-Tetrol from Bio-Renewable Levoglucosanol in Water: Effect of Metal and Acid Sites on (Stereo)-Selectivity. *Green Chem.* **2018**, *20* (19), 4557−4565.
(31) Stensrud, K.; Ma, C.c. Synthesis of R-Glucosides, Sugar Alcohols, Reduced Sugar Alcohols, and Furan Derivatives of Reduced Sugar Alcohols. US20170044123A1, 2017.
(32) Smith, B.; Ma, C. Process for the Isolation of 1,2,5,6-Hexanetetrol from Sorbitol Hydrogenolysis Reaction Mixtures Using Simulated Moving Bed Chromatography. US20170066702A1, March 9, 2017.
(33) Walker, T. W.; Motagamwala, A. H.; Dumesic, J. A.; Huber, G. W. Fundamental Catalytic Challenges to Design Improved Biomass Conversion Technologies. *J. Catal.* **2019**, *369*, 518−525.
(34) Chia, M.; O'Neill, B. J.; Alamillo, R.; Dietrich, P. J.; Ribeiro, F. H.; Miller, J. T.; Dumesic, J. A. Bimetallic RhRe/C Catalysts for the Production of Biomass-Derived Chemicals. *J. Catal.* **2013**, *308*, 226−236.
(35) Koso, S.; Ueda, N.; Shinmi, Y.; Okumura, K.; Kizuka, T.; Tomishige, K. Promoting Effect of Mo on the Hydrogenolysis of Tetrahydrofurfuryl Alcohol to 1,5-Pentanediol over Rh/SiO2. *J. Catal.* **2009**, *267* (1), 89−92.
(36) Koso, S.; Watanabe, H.; Okumura, K.; Nakagawa, Y.; Tomishige, K. Stable Low-Valence ReO $_x$ Cluster Attached on Rh Metal Particles Formed by Hydrogen Reduction and Its Formation Mechanism. *J. Phys. Chem. C* **2012**, *116* (4), 3079−3090.

(37) Koso, S.; Watanabe, H.; Okumura, K.; Nakagawa, Y.; Tomishige, K. Comparative Study of Rh−MoOx and Rh−ReOx Supported on SiO2 for the Hydrogenolysis of Ethers and Polyols. *Appl. Catal., B* **2012**, *111−112*, 27−37.
(38) Tamura, M.; Yuasa, N.; Cao, J.; Nakagawa, Y.; Tomishige, K. Transformation of Sugars into Chiral Polyols over a Heterogeneous Catalyst. *Angew. Chem., Int. Ed.* **2018**, *57* (27), 8058−8062.
(39) Cao, J.; Tamura, M.; Nakagawa, Y.; Tomishige, K. Direct Synthesis of Unsaturated Sugars from Methyl Glycosides. *ACS Catal.* **2019**, *9* (4), 3725−3729.
(40) Cao, J.; Tamura, M.; Hosaka, R.; Nakayama, A.; Hasegawa, J. Y.; Nakagawa, Y.; Tomishige, K. Mechanistic Study on Deoxydehydration and Hydrogenation of Methyl Glycosides to Dideoxy Sugars over a ReO_x-Pd/CeO_2 Catalyst. *ACS Catal.* **2020**, *10* (20), 12040−12051.
(41) Zhou, M.; Krishna, S. H.; De bruyn, M.; Weckhuysen, B. M.; Curtiss, L. A.; Dumesic, J. A.; Huber, G. W.; Assary, R. S. Mechanistic Insights into the Conversion of Biorenewable Levoglucosanol to Dideoxysugars. *ACS Sustainable Chem. Eng.* **2020**, *8* (43), 16339−16349.
(42) Wan, H.; Chaudhari, R. V.; Subramaniam, B. Aqueous Phase Hydrogenation of Acetic Acid and Its Promotional Effect on P-Cresol Hydrodeoxygenation. *Energy Fuels* **2013**, *27* (1), 487−493.
(43) Olcay, H.; Xu, Y.; Huber, G. W. Effects of Hydrogen and Water on the Activity and Selectivity of Acetic Acid Hydrogenation on Ruthenium. *Green Chem.* **2014**, *16* (2), 911−924.
(44) van Putten, R.-J.; van der Waal, J. C.; de Jong, E.; Rasrendra, C. B.; Heeres, H. J.; de Vries, J. G. Hydroxymethylfurfural, A Versatile Platform Chemical Made from Renewable Resources. *Chem. Rev.* **2013**, *113* (3), 1499−1597.
(45) Heltzel, J.; Patil, S. K. R.; Lund, C. R. F.; Schlaf, M.; Zhang, Z. C. Chapter 5 - Humin Formation Pathways. *Reaction Pathways and Mechanisms in Thermocatalytic Biomass Conversion II: Homogeneously Catalyzed Transformations, Acrylics from Biomass, Theoretical Aspects, Lignin Valorization and Pyrolysis Pathways* **2016**, 105−118.
(46) Xiong, H.; Pham, H. N.; Datye, A. K. Hydrothermally Stable Heterogeneous Catalysts for Conversion of Biorenewables. *Green Chem.* **2014**, *16* (11), 4627−4643.

https://doi.org/10.1021/acssuschemeng.1c04759
ACS Sustainable Chem. Eng. 2021, 9, 16123−16132